Recent Progress of Low Voltage Circuit Breakers

MITSUBISHI ELECTRIC
Changes for the Better
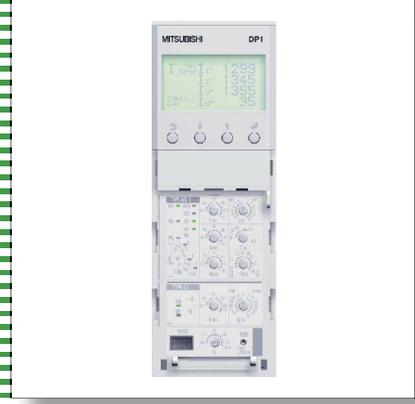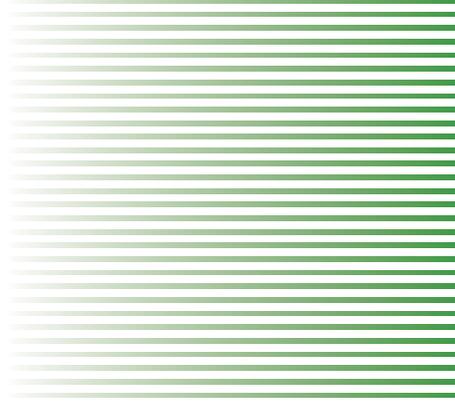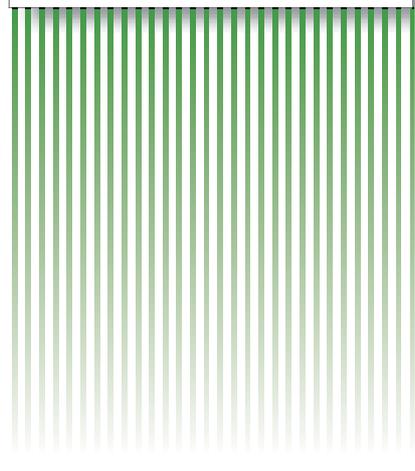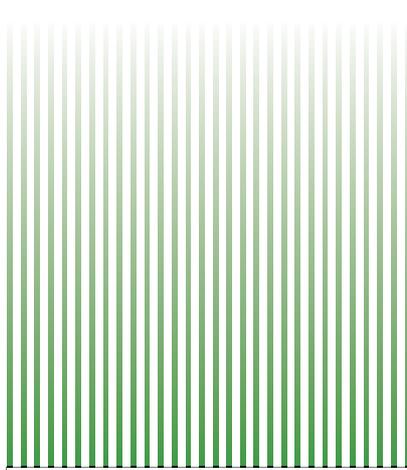
Cover Story

The globalization of markets, incorporation of intelligence, and mandatory implementation of environmental protection countermeasures are sweeping in waves over the field of low-voltage circuit breakers that protect electrical circuits from overload or short-circuits.

This feature issue introduces recent progress we have made with various kinds of low-voltage circuit breakers. The cover photograph shows one example of such developments.

CONTENTS

Technical Reports

Overview

Author: *Akira Sugiyama**

Electric power is an extremely convenient form of energy since it can be converted into a powerful driving force for huge machinery such as trains or into delicate signal waves for information communication, and into everything in between. It is indispensable to all countries, be they developing countries or industrialized countries that are home to the highly advanced information society. The low-voltage circuits carrying such electric energy are protected from overcurrent and short-circuit faults by circuit breakers, which have become ubiquitous, found without fail where electricity is used. As the consumption of energy grows in developing countries, the demand for low-voltage circuit breakers increases.

The feature papers in this edition describe new-model air circuit breakers developed for the global market, UL489-compliant small-sized molded case circuit breakers, measuring units for MDU breakers, efforts toward compliance with the RoHS Directive, and so forth, along with the new technologies that made these developments possible.

The low-voltage circuit breakers are one of the crucial infrastructures with which to supply power stably. At a time when global competition is becoming increasingly fierce, Mitsubishi Electric Corporation strives to continue supplying useful products to both domestic and global markets through persistent efforts at developing constituent technologies that anticipate future needs.

Low Voltage Air Circuit Breaker Type AE-SW Series

Authors: *Hiroshi Okashita** and *Kazunori Fukuya**

1. Product Overview and Features

The product line-up of the newly introduced AE-SW series air circuit breakers is shown in Table 1. The series comprises a total of nine models, from 630A to 4000A frames. Each model is available in the following four different kinds of outline modules: fixed type, drawout type, 3-pole type, and 4-pole type.

Major features include:

(1) The compact-sized AE2000-SWA model has been added.

(2) Thanks to extended operating durability, high reliability is achieved (mechanical durability has been increased from 10,000 to 25,000 cycles for 630 through 1600 AF).

(3) By virtue of increased high-voltage breaking capacity, superior short-circuit protection performance has been achieved (from 50 kA to 65 kA at AC 690 V for 630 through 2000 AF, and from 50 kA to 75 kA at AC 690 V for 2000 through 4000 AF).

(4) On the strength of enhanced short-time withstand performance, the coordination range has been expanded (from 65 kA to 75 kA in terms of 1-second duration values for 2000 through 3200 AF).

(5) The enhancement of insulation resistance has resulted in a higher safety. (The rated impulse withstand voltage of the main circuit has been increased from 8 kV to 12 kV.)

(6) Retrofitting to existing previous models is possible.

(7) Electronic trip relays that are capable of flexibly meeting wide-ranging customer needs.

2. Compact-sized AE2000-SWA

The newly introduced AE-SW-series 2000A frame products are available in two models: (1) AE2000-SWA (compact-sized type) and (2) AE2000-SW.

The compact-sized AE2000-SWA has been downsized to the 1600A-frame outline dimensions, along with a reduction in weight, in order to reduce the panel size.

As for rated breaking capacity and rated short-time withstand current specifications, we decided to adopt a performance rating of 65 kA, which is on a par with comparable specifications for 1600A-frame products.

Figure 1 shows the conductor structure of the ACB.
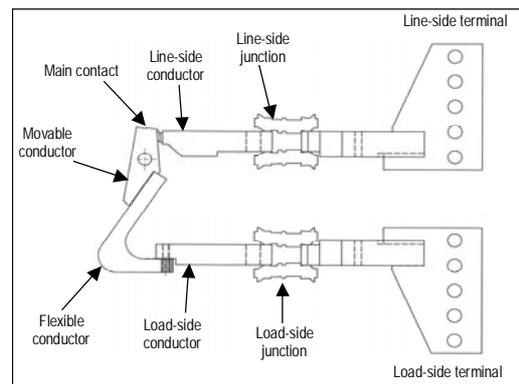
Fig. 1 Conductor structure of air circuit breaker

From the line-side terminal, current passes through the line-side junction, line-side conductor, main contact, movable conductor, flexible conductor (thin copper plate), load-side conductor, load-side junction and load-side terminal, in that order.

Temperature rise in various portions of the ACB are ascribable to Joule heat generated by the specific resistance of each individual part and the contact resistance at the junctions, connections and contacts. Finding ways to reduce these resistances present an important challenge to us.

The major measures we have taken to suppress temperature rise are enumerated below:

(1) An increase in the conductor cross-sectional area of the flexible conductor (thin copper plate)

(2) Reduction in contact resistance by virtue of increased contact surfaces of the junction connections

(3) Securing of shear planes in the connector junctions by means of high-precision fine blanking of the contact surfaces of the connections

(4) Vertical embedding of the conductors on the cradle

Table 1 AE-SW-series product line-up

A	630	1000	1250	1600	2000	2500	3200	4000
AE-SW series	AE630-SW	AE1000-SW	AE1250-SW	AE1600-SW	AE2000-SWA			
					AE2000-SW	AE2500-SW	AE3200-SW	AE4000-SWA

(5) An increase in the conductor cross-sectional area (plate thickness) of the central pole conductor on the cradle

In order to grasp the efficacy of the measures taken, we performed thermal analysis by means of a thermal circuit network. (See Figs. 2 and 3.)

As a result, we could quantitatively estimate the temperature rise that would be achieved with improved contact resistance, specific resistance and thermal dissipation in individual places without the need to perform temperature-rise testing on actual air circuit breakers on a measure-by-measure basis. This approach proved useful in narrowing down effective measures. On the aforementioned specifications concerned with the measures implemented, we verified that they were within spec by checking efficacies represented by the thermal circuit network and also by performing temperature-rise testing on actual air circuit breakers.

3. Enhancement of Operating Durability

The number of operating cycles for the newly introduced AE-SW-series air circuit breakers has been increased from 10,000 to 25,000 cycles for 630 to 1600A frames and from 10,000 to 20,000 cycles for 2,000 to 4,000A frame, thereby attaining the world's highest operating durability performance.

Figure 4 shows a cross-sectional view of the ACB, and Figs. 5 through 7 show operating stages of the mechanical section and the conductor section. Since impulsive load acts on each individual part with energy stored in the closing spring at the time of closing operation, the securing of rigidity and reliability of each individual part poses an important challenge to us for an improved number of operating cycles.

Below, we describe technical issues and their solutions:
(1) Quantification of impulsive load acting on each part
(2) Establishment of a margin of safety for each target operating cycle count
(3) Collection and organization of S-N curve data on candidate materials
(4) Establishment of a design technique that takes the notch factor of shaft parts into consideration

As for the measurement of impulsive loads, we employed distortion gauges for quantification. Taking into consideration variation in materials, we set an allowable repetition cycle count in relation to the target cycle count and established a margin of safety in relation to the fatigue limit of materials.

As to candidate materials for adoption into mechanism sections, we performed repetitive fatigue testing of test pieces and built and a reference databank of S-N

Fig. 2 Thermal circuit network of AE2000-SWA
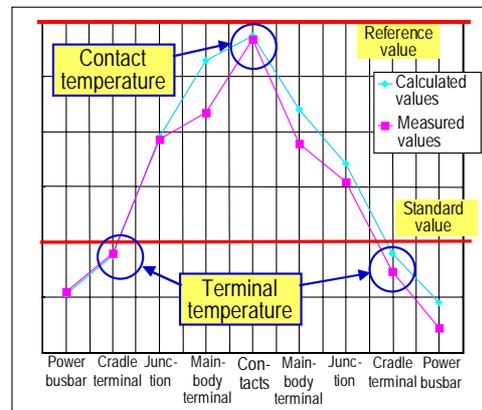
Fig. 3 Results of calculations and actual measurements on thermal circuit network

Fig. 4 Cross-sectional view of ACB construction
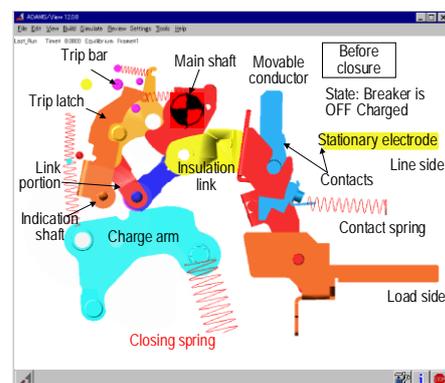
Fig. 5 ACB in the OFF position & in a charged state
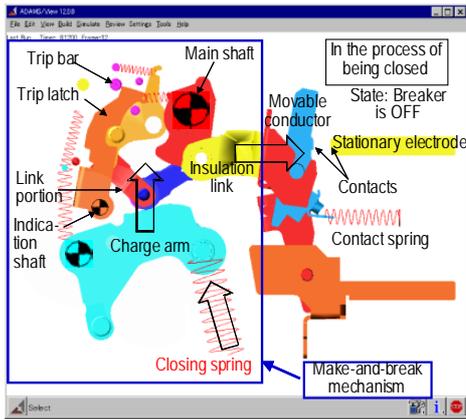
Fig. 6 ACB in the process of being turned ON
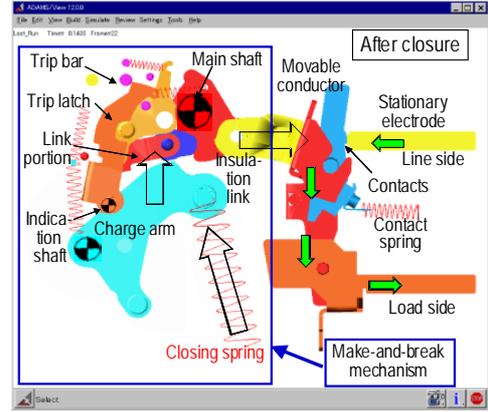
Fig. 7 ACB in the ON position & in a discharged state
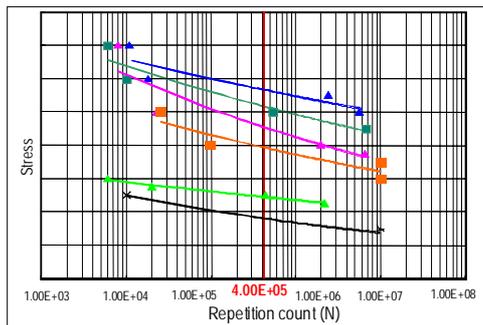
Fig. 8 S-N curves of candidate materials for mechanisms

<Calculation results>

Part name:	Indicator shaft						
	Material	Rotational bending stress	Thicker diameter D	Thinner diameter d	Fillet radius p	Generated stress rate	Safety margin
Before taking measures	A	○	10	9.6	0.1	100	○
After taking measures	R	◉	13	12.4	0.1	50	◉
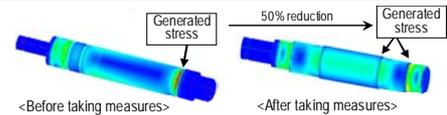
Fig. 9 Results of calculation and CAE analysis factoring in shape coefficients

curve data.

Where shaft parts are concerned, on the strength of the design technique that takes the notch factor into consideration, we implemented the optimization of shape-study and materials-selection procedures designed to achieve the safety margins that we established. By virtue of the study flows that we implemented to secure the rigidity and reliability of each individual part, we successfully increased operating-cycle counts significantly. (See Figs. 8, 9 and 10.)

4. Electronic Trip Relay

As to electronic trip relays for the newly introduced AE-SW-series units, we achieved the development of electronic trip relays capable of meeting diverse requirements by selectively combining various kinds of modules with one common ETR base equipped with basic tripping functionality.

The lineup of these various modules is as follows:
(1) Main setting modules, each of which incorporates an overcurrent-protection characteristic tailored to a specific application
(WS: General use, WM: Generator protection use, WB: Special use)
(2) Optional setting modules, each of which incorporates optional functionality such as ground-fault protection or a 2nd additional pre-alarm
(G1: Ground-fault protection, N5: Neutral pole 50% protection, E1: Earth leakage protection; AP: 2nd

Fig. 10 Rigidity and reliability study flow

pre-alarm)
(3) Power supply units (available in 5 kinds) designed to supply power to trip indicator LEDs, extension modules etc.
(4) Extension modules for measuring current, voltage, power etc.
(5) Displays for indicating measured values, alarm information, etc.
(6) Interface units for making connections to various field networks
(7) I/O units for remotely controlling circuit breakers

We have thus far discussed the major features of the newly introduced AE-SW-series air circuit breakers.

In the future, we are determined to continue offering air circuit breakers oriented toward customer satisfaction.

Optimum Design of Short-Circuit Electromagnetic Forces of Multi-Finger System in Low Voltage Circuit Breaker

Authors: *Yo Makita*[*] and *Toshie Takeuchi*[*]

With the objective of stepping up the rated short-time current resistance of the new-type AE-ES-series air circuit breakers, we established a design method in which an A-ϕ-formulation-based three-dimensional transient electromagnetic field analysis technique is introduced. The technique lends itself to the consideration of non-uniform current distribution in main-circuit conductors. The results of optimization using this design method on a main-circuit construction demonstrated that we have successfully achieved an increase in grade for two models (AE2000-SW and AE4000-SWA) in rated short-time current resistance.

1. Short-time Current-resistant Design Technique for Main-circuit Portions

1.1 Transient Electromagnetic Analysis Model and Analytical Technique

Figure 1 shows a cross-sectional view of the main circuitry construction of our air circuit breakers (ACBs). The main circuitry consists of the line-side fixed conductor to which the fixed contact is fixed, the movable conductor to which the movable contact is fixed, the flexible conductor made up of laminated thin copper plates, and the fixed load-side conductor. The movable conductor and flexible conductor are each made up of multiple fingers and are connected with the link pin on a phase-by-phase basis.

To consider non-uniform current distribution in conductors due to the skin effect at the time of short-time current-resistant energization, we employed EMSolution (general-purpose software developed by Science Solutions International Laboratory Inc.), which adopts a transient electromagnetic field analysis technique based on the finite element method of the A-ϕ formulation using edge elements.

Since this particular technique uses electric scalar potential ϕ and magnetic vector potential A, it is capable of dealing with skin effects that take place on various kinds of materials. In addition, for the calculation of electromagnetic forces generated on the individual portions of the finger conductors, we adopted the nodal force method that makes it possible to determine the electromagnetic forces of individual elements with ease and precision. Figure 2 shows analysis meshes that are a model representation of the three-phase main circuitry of an ACB. In order to accurately analyze the impact of eddy currents that are generated in the main-circuit portions at the time of short-time current-resistant energization, each conductor is composed of meshes having a thickness that is less than one third the thickness of the skin (= 8 mm at 60 Hz). By dividing each flexible conductor into 10 parts in the lamination direction and splitting each finger into 5 parts in the direction of the side-by-side arrangement, we created the above model,


Fig. 1 Cross-sectional view of the construction of ACB main circuitry
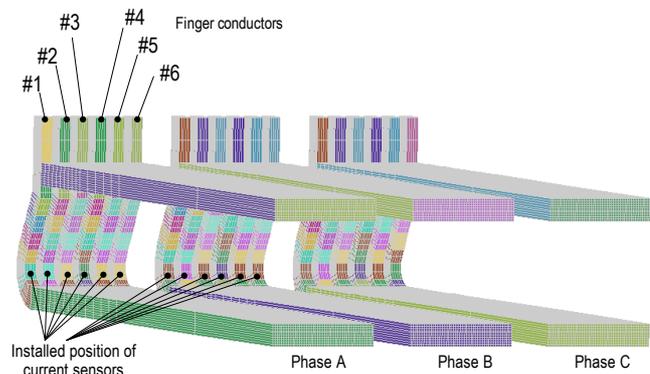
Fig. 2 Mesh model of the main circuitry of AE4000-SWA

* *Advanced Technology R&D Center*

which is made up of approximately 300,000 elements including air regions. Furthermore, in order to impart electric scalar potential ϕ, which determines the total amount of current flowing into the surfaces of conductors, we pasted surface elements onto the surfaces of the line-side fixed conductors of each phase. For input current, we used actual amperage values derived from 80-kA three-phase short-circuit current energization testing, capable of causing up to 190 kA in peak current to flow into Phase A and Phase B.

1.2 Short-time Current-resistant Performance Enhancement Design Technique

Next, using Fig. 3 (a), we discuss the generation mechanism of contact pressure in the contact region. When current flows through the main circuitry, electromagnetic force $Ffin$ generated on the flexible conductor and contact pressure spring force Fsp combine to work as pressing force (contact pressure) Fpr with the link pin serving as a fulcrum. In the figure, although the location of $Ffin$ generation is represented by a single point, actual electromagnetic force is widely distributed over the entire electrical path. For this reason, as shown in Eq. (1), Fpr is the sum total of individual electromagnetic forces $Ffin_i$ as determined by electromagnetic analysis on individual elements.

$$Fpr = \sum_i Ffin_i \frac{Lfin_i}{Lcon} + Fsp \frac{Lsp}{Lcon} \qquad (1)$$

Where $Lfin_i$ = the distance between the point of application of electromagnetic force of the element i in the electrical path and the link pin, Lsp = the distance between the point of application of contact pressure spring force and the link pin, and $Lcon$ = the distance between the point of application of contact repulsive force and the link pin.

On the other hand, electromagnetic repulsive force $Fcon$ simultaneously occurs in the contact region due to current concentration. Even though this electromagnetic repulsive force may be determined, generally, with the help of Holm's formula, this approach leaves the problem of precision because approximations are made to determine the contact area of the contact. Since it is important to grasp the repulsive force with a high degree of precision in order to implement optimum short-time current-resistant performance enhancement design, we conducted testing on a model representing an extracted contact region and determined the contact region's repulsive force $Fcon$ from the results of measurement to determine the current dependence of the electromagnetic repulsive force.

To achieve good short-time current-resistant performance, our aim is, therefore, to develop a design such that the contact pressure Fpr becomes greater than the contact region's electromagnetic repulsive force $Fcon$ at all times during energization. Here, we define the differential between Fpr and $Fcon$ as a margin of contact pressure. The greater the margin of contact pressure, the better the short-time current-resistant performance. As the simplest way to increase Fpr, we considered increasing the contact pressure spring force Fsp. However, this would place a greater load on the contact-making mechanism and, thereby, give rise to reliability-related problems such as increased contact-making impacts. Given this situation, our aim was to achieve stable short-time current-resistant performance by improving the geometries of the movable conductor without increases in contact pressure spring force, as shown in Fig. 3.
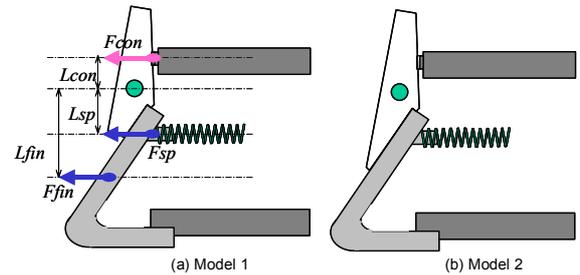
Fig. 3 Cross-sectional views of prototype models

2. Three-dimensional Transient Electromagnetic Field Analysis

Figure 4 shows the results of current-density analysis conducted 6 ms after commencement of energization. As can be seen, the currents flowing in the individual fingers are not uniformly distributed in density and the outermost fingers are carrying the heaviest concentration under the influence of eddy currents. In particular, a closer inspection reveals that Phase-A Finger #6 lying immediately next to Phase B and Phase-B Finger #1 are carrying approximately two times the current of the fingers taking up the inner positions under the influence of Phase-A and Phase-B magnetic fields, respectively. Here, please take note that this analytical method is a relatively new technique employing a surface current definition method. Although the method has a track record[3] of short-circuit electromagnetic force analyses on high-voltage power equipment, no comparison has heretofore been made for verification purposes between the method and real-world experiments in terms of the precision of current distribution in multi-finger structures. Given this situation, we placed Rogowskii coils on the individual fingers of Phases A and B as shown in Fig. 2 to measure time-varying currents that flow through those fingers. We obtained results indicating good agreement between analytical values and corresponding actually measured values within 10% in both Phase A and Phase B. Furthermore, the current waveforms of the individual fingers were also in good agreement with one

another. From this, the analytical technique has been confirmed to have adequate precision. From the fact that the time-varying current distribution was able to be analyzed with accuracy as discussed above, we conclude that the electromagnetic force of each finger, as calculated from the interaction between the current and the magnetic field, also has adequate precision.
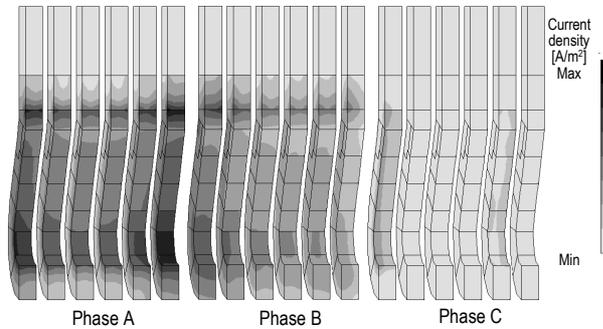
Fig. 4 Current density distribution among finger conductors (6 ms after commencement of energization)

3. Short-time Current-resistant Performance Enhancement Design Results

On prototype Models 1 and 2 shown in Fig. 3 in the preceding chapter, we performed short-time current-resistant performance enhancement design using contact pressure and repulsive force determined from analysis conducted on each contact. As for the contact repulsive forces, we used actually measured repulsion values obtained from testing performed on the contact-region models by passing currents through the individual fingers, the amperage of which is equal to the current values determined from this analysis. In the case of prototype Model 2, a main-circuit structure is adopted that lends itself to better use of the electromagnetic force generated in the flexible conductor as contact pressure. We believe that the electromagnetic force generated in the flexible conductor at the time of energization actively contributes to serve as contact pressure in the region where contact is made with the movable conductor. However, we do not believe that this force effectively contributes in places other than the contact-making region. In the case of the short-time current-resistant performance enhancement design, we assumed that contact pressure works effectively in the contact-making region only, where the movable conductor and the flexible conductor are in perfect contact with each other in order to more safely secure a contact pressure margin.

Figure 5 shows the relationship between the contact pressure and the repulsive force in Phase A for both prototype Models 1 and 2 obtained from the experimental results. In the case of prototype Model 1, the contact pressure is greater than the repulsive force on Phase-A Finger #1 while the difference between the

contact pressure and the repulsive force is extremely small on Phase A Finger #6 in the neighborhood of 6 ms where Phase B peak appears, indicating that there is a possibility not to secure a contact pressure margin. In other words, Phase-A Finger #6 may arc in the neighborhood of 6 ms and, thereby, prevent the short-time current-resistant performance from being achieved. By contrast, in the case of prototype Model 2, the contact pressure is always greater than the repulsive force during energization. Since a sufficiently large margin of contact pressure is secured, favorable short-time current-resistant performance can be achieved.
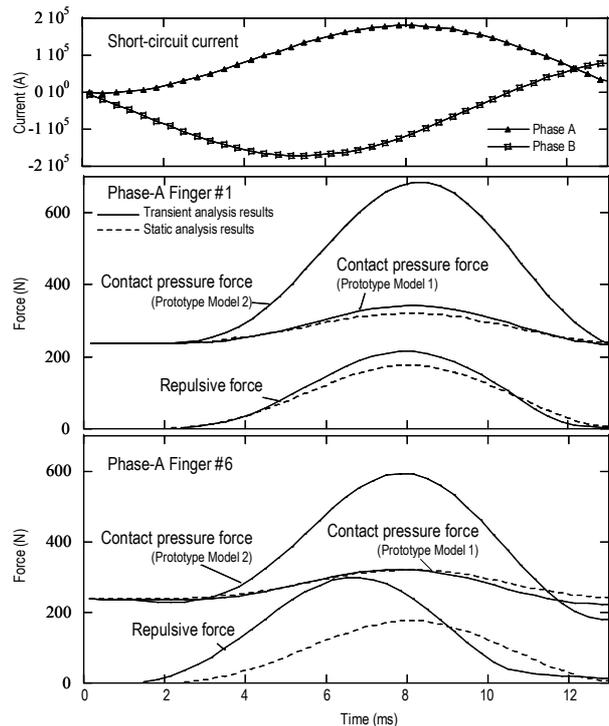
Fig. 5 Contact pressure and repulsive force of Fingers #1 and #6

Based on the above results, it has been shown that the shape of the tail end of the movable conductor contributes heavily to the enhancement of the contact pressure. This leads us to consider that, by adopting an optimum tail-end shape, it is possible to efficiently convey the electromagnetic force of the flexible conductor as contact pressure and, thereby, achieve stable short-time current-resistant performance.

For reference, short-time current-resistant performance enhancement design results derived from prototype Model 1, which was fabricated based on previously used static magnetic field analysis, are shown in the form of broken lines in Fig. 5. In the case of the static magnetic field analysis, the overlap between the contact pressure and the repulsive force observed 6 ms after the commencement of energization in the aforementioned transient electromagnetic field

analysis is not seen. This is considered to be ascribable to the following reason: Since it is impossible to give consideration to eddy current-caused uneven flows of current among the fingers, it is simply taken for granted that one sixth of Phase A's total current flows through Phase-A Finger #6, a smaller current than that determined by the aforementioned transient analysis. The repulsive force generated at the contact is considered to thus become weak.

Finally, we conducted short-circuit testing on both prototype Models 1 and 2 by passing 80 kA, which includes some specification margin with respect to the AE4000-SWA's rated short-time current resistance of 75 kA. (Model AE4000-SWA is an air circuit breaker with a rated current of 4000 A.) As a result, prototype Model 1 arced at 80 kA on Phase-A Finger #6 while prototype Model 2 featuring an improved movable conductor shape satisfactorily demonstrated good short-time current-resistant performance without arcing and, thereby, proved that we have achieved our

short-time current-resistant performance enhancement objective. The fact that the results agreed with the aforementioned short-time current-resistant perform-ance enhancement design results is considered to indicate the validity of the design technique we adopted this time around. Furthermore, although we conducted short-time current-resistant performance enhancement design and assessment on the AE4000-SWA in con-junction with this paper, the improved movable con-ductor structure is effective for all other capacity ratings. Also with the AE2000-SW (with a rated current of 2000 A), we have confirmed the achievement of similar im-provements in short-time current-resistant performance.

Since the design technique established this time around is applicable irrespective of conductor geome-tries and current ratings, we intend to promote the widespread application of the technique to enhance the reliability of high-current carrying performance in future air circuit breakers.

Electronic Trip Relay for Low Voltage Air Circuit Breaker AE-SW Series

Authors: *Koji Hirotsune** and *Toshimitsu Nomura**

As electronic trip relay features for use with low voltage air circuit breakers (hereinafter called "ACBs"), we have developed add-on-type electronic trip relays for use with the newly introduced AE-SW-series ACBs, which are capable of flexibly meeting diverse specifications when selectively coupled to provide a range of functions such as the following various protection functions, the capability to measure, display and transmit about the circuit, the function to alarms output signals, and the ability to remotely control the ACB.

1. Add-on-type Electronic Trip Relays for AE-SW ACBs

The add-on-type electronic trip relays can be divided into the ACB's ETR base module and an additional function module for such purposes as measurement and transmission.

The ACB's ETR base module consists of an ETR base which realizes a trip function, a main-setting module with which to set overcurrent protection, an optional-setting module with which to set ground-fault protection and the like, an alarm contact output function, and a power supply module that incorporates a control-circuitry power supply.

Each additional function module consists of an extension module to perform the measurement of current, voltage, power and the like, a display to indicate measurement values and the like, an interface unit for field networking purposes, an I/O unit for the purposes of remotely controlling the ACB, and the like.

By breaking down relay functionality into functional modules and by allowing selections and combinations to be freely made from among those modules, it becomes possible to flexibly satisfy diverse relay specifications.

2. Specifications and Features of ACB's ETR Base Module

As shown in Fig. 1, the ETR base module consists of the ETR base, the main-settings module, the optional-settings module and the power supply module.

The main-settings module with which to set overcurrent protection is available in three kinds: general use (WS), generator protection use (WM) and special use (WB). By combining one of these with the ETR base, overcurrent protection, which is a basic function,

becomes possible.
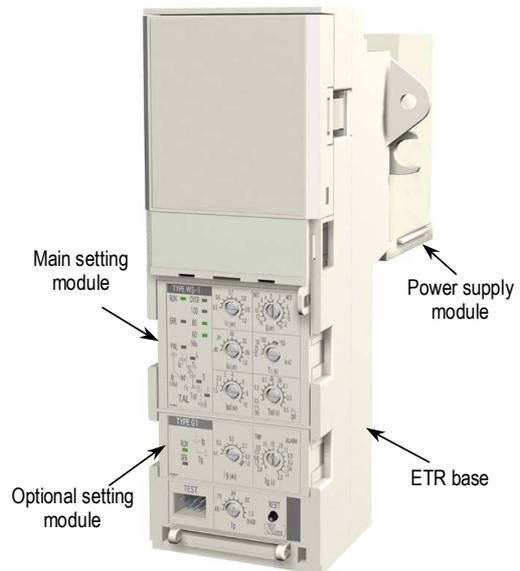
Fig. 1 Electronic trip relay

By adding optional-settings modules, which are optionally available for the ETR base, various kinds of protection become possible. There are four different kinds of optional-settings modules to choose from: Ground-fault protection (G1), Earth-leakage protection (E1), 2nd additional pre-alarm (AP), and Neutral pole 50% protection (N5).

Assembling various combinations of the main-settings module and optional-settings modules enables realization of diverse tripping functions such as those shown in Table 1.

The power supply module supplies power to the trip indicator LEDs incorporated in the main-settings module and the optional-settings module, the contact output circuit installed in the power supply module, the ETR circuit, and additional function modules such as the extension module that we discuss later on. The lineup of power supply modules is shown in Table 2.

3. Specifications and Features of Additional Function Modules

The product lineup of the additional function modules is shown in Fig. 2. By installing the extension module at the back of the ETR base, it becomes possible to add abundant functions to the electronic trip relay.

Table 1 Characteristics table of ETR

	NA -	G1 Ground fault	E1 Earth leakage	AP 2nd Pre-alarm	N5 50% protection
WS LTD+STD+ INST/MCR					
WM LTD+STD+ INST/MCR					
WB INST/MCR					-

Table 2 Line-up of power supply modules

Type	Rating	Alarm output
P1	100-240V AC/DC	Nothing
P2	24-60V DC	Nothing
P3	100-240V AC 100-125V DC	6 output contacts
P4	24-60V DC	6 output contacts
P5	100-240V DC	6 output contacts by SSR

By virtue of incorporation of a newly developed measurement ASIC, the extension module is capable of a wide variety of measurement elements such as load current, voltage, power, harmonic currents up to the 19th harmonic, electric energy and the like with a high degree of measurement accuracy. To measure all measurement elements, the voltage-measurement VT unit is required. However, to measure current only, connection of a VT unit is not required. In addition, the capability to store history information on up to ten most recent fault and/or alarm occurrences is also incorporated.

What is more, as a means of transmitting values measured by the extension module to other units such as a display along with other information, we adopted the RS485's internal transmission scheme. Since the internal transmission protocol is capable of automatically performing hook-up recognition when units such as the display connection and the interface unit are connected to the internal transmission line, thus eliminating the need to perform setup work at the time of installing additional function modules and the like out in the field, the required functions can be added with
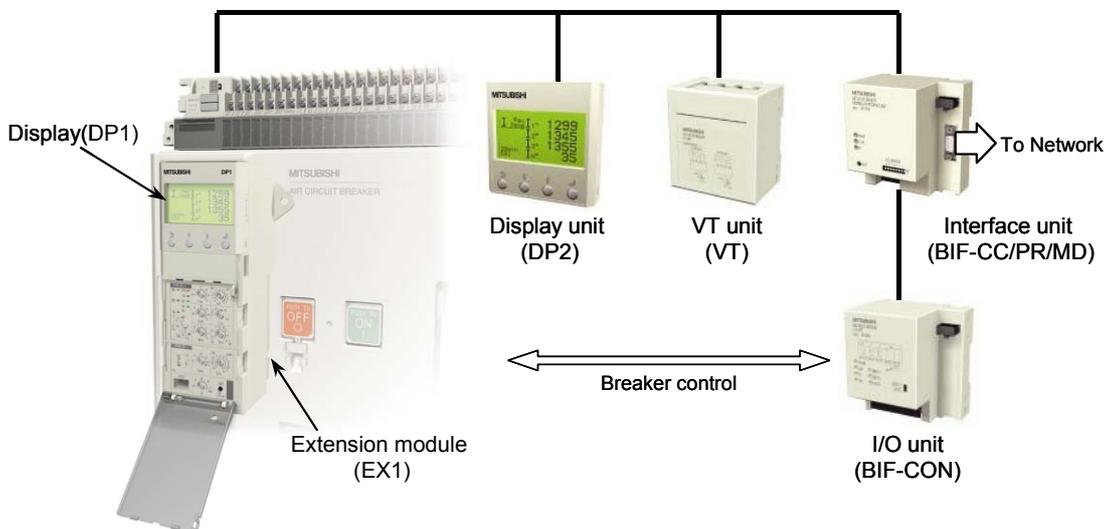
Fig. 2 Additional function module of ETR

ease.

As display modules to show various measured values, fault causes, history information, alarm information and the like, there are two kinds of display devices to choose from. One (DP1) is designed for installation at the front of the electronic trip relay and the other (DP2) is intended for installation on a panelboard. So long as a given electronic trip relay is equipped with the extension module, the function of the DP2 can be easily added through connection to the internal transmission connector located in the breaker control terminal section. Both DP1 and DP2 may be installed at the same time.

When there is a need to monitor various measured values, alarm information and the like by making a connection to various field networks, it is possible to connect an interface unit designed for each particular field network. The lineup of such interface units is shown Fig. 3.

Furthermore, by connecting both the interface unit and I/O unit (BIF-CON), remote control of the air circuit breaker becomes possible. The I/O unit incorporates dedicated "a" contact outputs that permit direct connections to a closing coil (CC), a shunt trip device (SHT) and a motor charge device (MD). Because of this provision, the air circuit breaker can be remotely controlled from a PLC (programmable logic controller), a SCADA (Supervisory Control And Data Acquisition system) or the like on a field network.

The new relays we have developed have considerable potential for expansion. Given this situation, we are committed to continually developing a group of modules that meet customer needs in order to foster greater flexibility for our ACB products.

CC-Link (BIF-CC) Profibus-DP (BIF-PR) Modbus: RS-485 (BIF-MD)

Fig. 3 Line-up of interface units

ASIC for Low Voltage Air Circuit Breaker AE-SW Series

Authors: *Toshimitsu Nomura** and *Kouichi Nishimura**

We have implemented in ASIC form the trip function circuit located inside the ETR base of the add-on electronic trip relay for use with the new AE-SW-series air circuit breakers and, thereby, achieved downsizing of the ETR. In this paper, we introduce this newly developed ASIC.

1. Composition of the Electronic Trip Relay for the AE-SW Series

The add-on electronic trip relay for use with the new AE-SW-series air circuit breakers consists of the ETR base, which realizes the trip function of the air circuit breaker, the main-settings module with which to make overcurrent protection characteristics settings, the optional-settings module with which to make ground-fault protection characteristics settings and the like, and a power supply module that incorporates trip/alarm contact output functions and a control-circuit power supply. Figure 1 shows an internal block diagram of the ETR.

The power to drive the trip coil of the air circuit breaker and to operate the newly developed ASIC is supplied from the power supply circuit after rectification by the rectifying circuitry of an output derived from a power supply CT mounted inside the circuit breaker. Furthermore, analog circuits as well as a microcomputer and its peripheral circuits inside the ASIC are energized by internal power supplied by the ASIC's constant-voltage circuit.

As for the principle of overcurrent detection, the output signals of coreless coils that are mounted inside the breaker to detect each phase's current are integrated, and the result is fed into an analog-to-digital converter in the microcomputer to perform effective-value calculation processing. For the ground-fault detection, the output signals of the coreless coils undergo integration and composition and the outcome is then processed in a manner much the same as that used for overcurrent detection. Furthermore, as to earth-leakage detection using an external ZCT, processing is performed in the microcomputer by way of earth-leakage circuitry.

2. Features of the ASIC for the New AE-SW-series Breakers

Figure 2 shows an internal block diagram of the
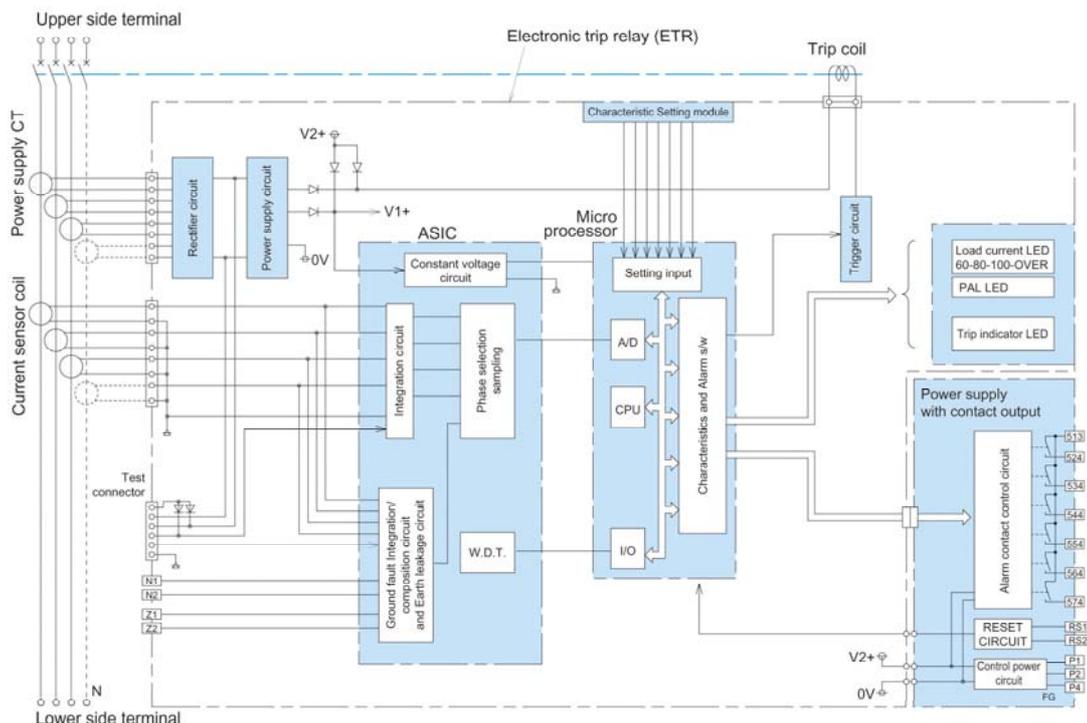
Fig. 1 Electronic trip relay circuit diagram

*Fukuyama Works

ASIC. The features of the individual circuit blocks are as follows:
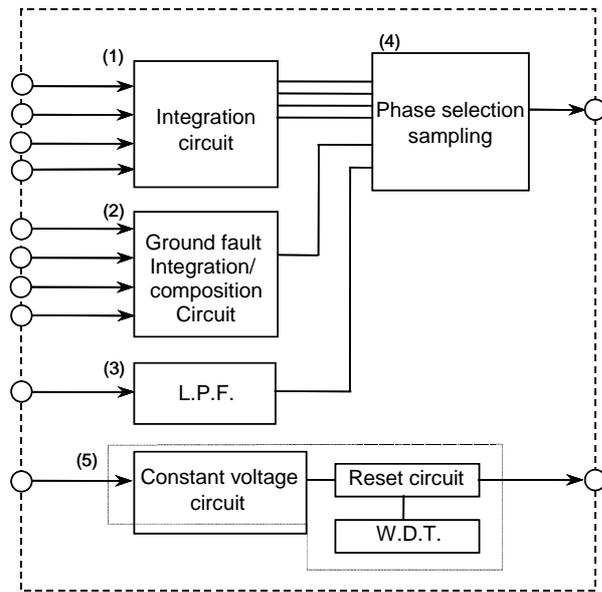
Fig. 2 ASIC diagram

(1) Overcurrent signal input circuit

The output waveforms of the coreless coils, each installed to detect the current of a phase, represent differentiated waveforms of the primary current waveforms. Circuits to integrate these differentiated waveforms and reconstitute them back into the original sinusoidal waveform are incorporated in the ASIC. What is more, the ASIC incorporates an integration circuit capable of use in three-pole breakers, each combined with an external N-pole CT (NCT) for neutral-pole protection purposes in a three-phase four-wire system.

(2) Ground-fault signal input circuit

For use as a ground-fault signal input circuit, the ASIC incorporates a ground-fault integration and composition circuit designed to perform vector composition and integration of the individual phase outputs of the overcurrent-detection coreless coils.

(3) Earth-leakage signal input circuit

The earth-leakage signal input circuit is equipped with a low-pass filter circuit to eliminate the harmonic content of the ZCT's secondary-side output signal. This filter makes it possible to effectively extract the fundamental component of earth leakage current and, thereby, permits stable earth-leakage detection.

(4) Phase selection sampling circuit

The analog output signals from the individual input circuits are fed into the analog-to-digital conversion block in the microcomputer for subjection to digital effective-value calculation processing. Here, overcurrent detection, ground-fault detection and earth-leakage detection for each phase use mutually independent effective-value detection methods. For the purpose of

switching among the individual signals for outputting to the analog-to-digital converter, the ASIC incorporates the phase selection sampling circuit.

(5) Constant-voltage circuit

The power to the ASIC's internal circuits, namely the microcomputer and peripheral circuits, is supplied from the ASIC's constant-voltage circuit. Since this constant-voltage circuit incorporates a microcomputer reset circuit, stable operation can be obtained. Moreover, in addition to a watchdog timer built inside the microcomputer for the purpose of monitoring a possible program runaway, a watchdog function is also embedded in the ASIC to doubly ensure stable operation.

3. Features of the ASIC and Its Peripheral Circuitry

In the breaker's overcurrent trip operation, the maximum breaking time of instantaneous trip operation is 40 ms or shorter. If a short-circuit fault occurs in a state where no power is supplied to the electronic trip relay, for example, at a time when the breaker's load current stands at 0 A, the electronic trip relay should ready itself to trip in the shortest possible time after it has begun receiving power from the power supply CT. To this end, the time required for the power to rise has been shortened by reducing the current draw of the ASIC itself. The power consumption reduction of the ASIC itself was intended to ensure that tripping operation can be successfully performed even when the GFR pickup current is set to $0.2 \times In$ (CT rating).

What is more, to shorten the relay's operation time, the constant-voltage circuit in the ASIC has been designed to ensure that it builds up power and puts it out fully in 300 μs at the longest. Moreover, the operating voltage for the microcomputer and its peripheral circuitry used for the AE-SW-series breakers developed this time is a mere DC 3.3 V. The use of this low voltage also contributes to the reduced current consumption.

By mounting the ASIC incorporating the above-mentioned features in the ETR bases of electronic trip relays for the AE-SW-series breakers, it has become possible to not only reduce electronic trip relay dimensions but also commercialize a variety of function-specific electronic trip relays from which to choose.

Figure 3 shows a conventional electronic trip relay for AE-SS-series breakers and the newly developed electronic trip relay for the AE-SW-series breakers for comparison of their external appearances. Although the figure shows the electronic trip relay portions only, a 50% reduction has been achieved in terms of surface-area ratio.

AE-SS series   AE-SW series
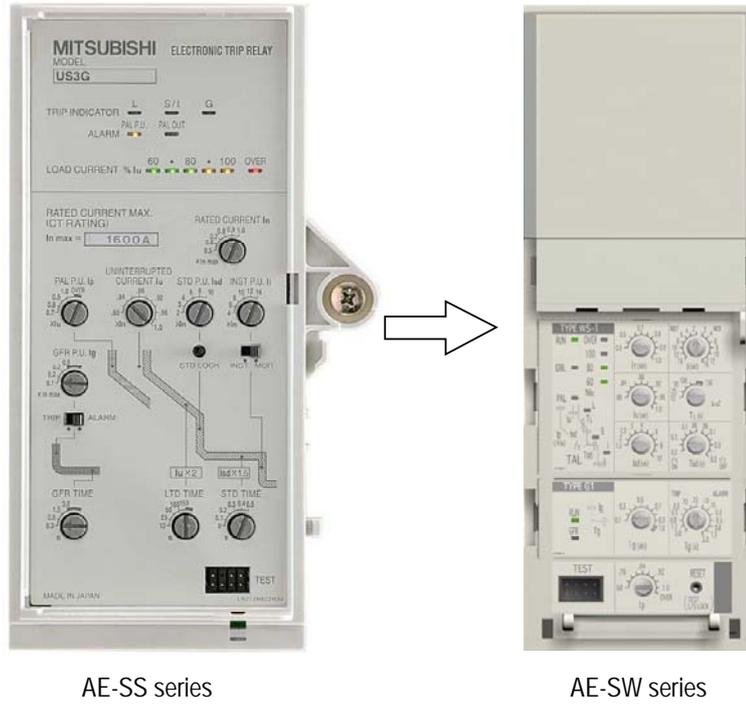
Fig. 3 Electronic trip relay

In conclusion, a photo of the newly developed ASIC is shown in Fig. 4. This IC measures 12 mm by 12 mm by 1.85 mm and is encapsulated in a 64-pin QFP (quad flat package). The ASIC is also suitable for lead-free soldering.
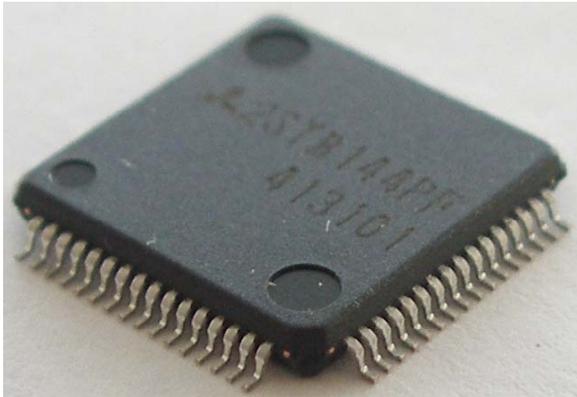

Fig. 4 ASIC

UL489 Listed Molded Case Circuit Breaker "SRU/HRU" Series

Authors: *Toshiyuki Tanibe*[*] and *Susumu Takahashi*[*]

In a bid to address the need for smaller-sized multi-standard circuit breakers that are compliant with the UL489 standard and are capable of being used in 480-V delta circuitry, we have been working on the development of the "SRU/HRU" Series (Fig. 1).

In this paper, we describe the major features of the SRU/HRU Series along with the new technologies that we developed to realize those features.

1. New Technologies Making Downsizing Possible

1.1 Linear-motion Double-breaking Technology

In the case of machinery and equipment destined for export to North America, the incorporated circuit breakers should be recognized under UL489. Since this standard differs from IEC and JIS standards and it was extremely difficult to achieve downsizing using conventional breaking construction, we adopted a linear-motion double-breaking system as a new breaking method (See Fig. 2). As a general rule, a large spacing distance is required to interrupt a high voltage. By virtue of the use of the above-mentioned construction, it has become possible to not only effectively increase the contact-to-contact distance but also to achieve high-speed pole-opening operation. As a result, it is possible to break contact in a space that is smaller than the comparable space of a typical single-breaking system. Furthermore, the construction in which the arc-extinguishing chamber responsible for breaking contact and the make-and-break mechanism plus the

overcurrent trip relay are separated from each other by the inner wall of the breaker, contributes to the enhancement of insulation and the operation reliability of the make-and-break mechanism at the time of short-circuit-caused breaking.

1.2 New Small-sized Mechanism

In order to pack all functions into a limited space inside the breaker and, thereby, achieve reduced dimensions, the mechanism section had to be downsized as well. With this being the situation, departing from our conventional toggle link mechanism, we made the following structural changes/modifications and developed a new small operating mechanism having about the same driving force as that of its predecessors (See Fig. 3).

(1) The frame-to-frame spacing distance was reduced, and the closing spring was placed outside the frame while the link mechanism was placed in between the frames.

Because of the reduced frame-to-frame spacing, each individual link part was fixed in place with a pin at short spans. As a result, it has become possible to reduce stress on the pins. Since the diameter of each pin could be decreased commensurate with the decrease in stress, the link parts could also be downsized.

(2) The pin on which the closing spring is engaged is guided by a groove formed in the frame. This pin is arranged so as to be driven by the handle.

**Fig. 1 UL489 listed molded case circuit breaker "SRU/HRU" series**
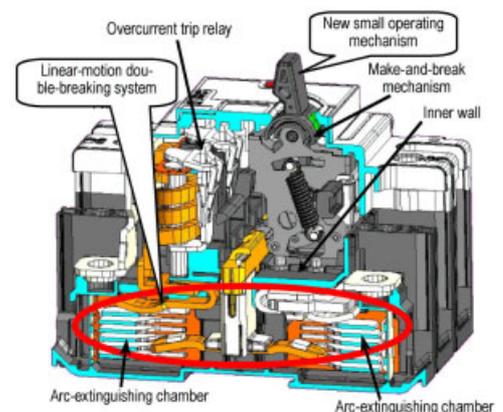
Fig. 2 Internal construction of NF100-HRU

*Fukuyama Works
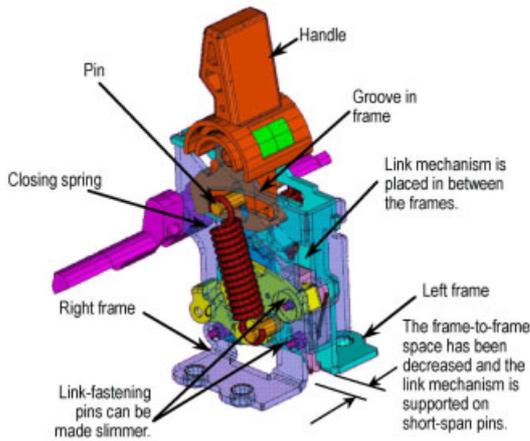
Fig. 3 Parts layout of new operating mechanism

The closing spring is driven at the center of an arc-shaped groove formed in the frame. Since it is possible to change the position of the rotation center of the handle and the center of the pin's track, we could achieve a mechanism section characterized by a small window frame for the handle.

As a result, we were able to develop a small-sized slim mechanism section with a volume that is about 40% of that of comparable conventional 100A frames. On the strength of the above newly developed technologies, where UL489-compliant circuit breakers capable of use in 480-V delta circuitry are concerned, we have achieved considerable downsizing, approximately 60% reduction in volume compared to our conventional model (NF-SFW), as shown in Fig. 4.
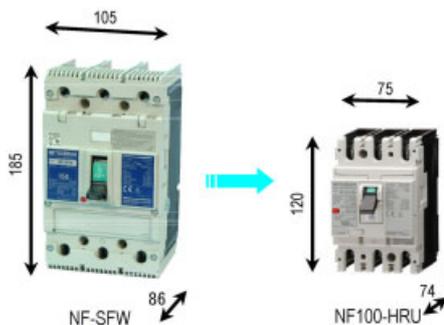

Fig. 4 Reduction in volume to 40% of that of the our conventional model

2. Enhancement of Ground-fault Protection Capability by the Addition of Type-A Residual Current Characteristics

In recent years, the use of equipment incorporating such rectifying circuitry as inverters and servos has been increasing in the interest of enhancing the precision of drive control. If the rectifying circuit of such equipment fails, there are cases in which there is a flow of leakage current having a half-wave rectified waveform. In order to make it possible for a circuit breaker to detect this leakage current and, thereby, trip to prevent

an electric shock and/or leakage current-caused fire, it is necessary to equip the circuit breaker with Type-A residual current protection characteristics shown in Table 1 (as stipulated in EN 60947-2). To this end, we have incorporated a newly developed digital/analog mixed-signal ASIC into our SRU/HRU-series Molded Case Circuit Breakers with ground-fault protection to not only broaden the scope of ground-fault protection made possible with the Type-A characteristics but also achieve the downsizing of electronic circuitry.

Table 1 Operating characteristics of residual current

	AC residual current waveforms	Half-wave rectified residual current waveforms
Type A (SRU/HRU Series)	○ Capable of detection	○ Capable of detection
Type AC	○ Capable of detection	✕ Incapable of detection

3. Reduction in Environmental Load Through Adherence to RoHS Directive

At a time when the world is clamoring for tougher regulations and controls over emissions of harmful substances, the most famous one is the RoHS Directive (Restriction of the Use of Certain Hazardous Substances in Electrical and Electronic Equipment Directive), which stipulates that, from July 1, 2006, new electrical and electronic equipment put on the market should not contain lead, mercury, cadmium, hexavalent chromium, polybrominated biphenyls (PBB) or polybrominated diphenyl ethers (PBDE). By virtue of the following measures (1) through (4), the SRU/HRU-series breakers comply with the RoHS Directive. Since these measures were implemented on not only the breakers themselves but also on accessory devices, the entire works of the SRU/HRU series are fully compliant with the RoHS Directive.

(1) Reduction in solder joints and soldered places and the use of lead-free solder

For conventional products, solder was used even to fasten structural components in some places. Design changes have been made to eliminate such places. In the case of the Molded Case Circuit Breakers with ground-fault protection, solder is being used in their electronic circuitry. However, all soldering is done using lead-free solder.

(2) Adoption of cadmiumless contacts

Although some conventional breaker contacts contain cadmium, the contacts used in the SRU/HRU-series breakers are 100% cadmium free.

(3) Replacement of hexavalent chromium with triva-

lent chromium

In the past, hexavalent chromium was widely used for chromate treatment of zinc plating. In the case of the SRU/HRU-series breakers, we abolished all use of hexavalent chromium and began using trivalent chromium for chromate treatment of all zinc-plated parts including small screws.

(4) PBB and PBDE

Both of these substances are added to plastic materials to render them flame retardant. However, the SRU/HRU-series breakers use no plastic materials that contain these substances.

4. Internationalization of Breakers Through Adherence to Multiple Standards

Nowadays, globalization is proceeding rapidly in every aspect the world over. Companies that manufacture machinery and equipment for exportation to vari-ous countries have a particularly strong need for components that incorporate/satisfy multiple standards for installation into their products. In addition to meeting the U.S.'s UL489, the SRU/HRU-series breakers satisfy all standards shown in Table 2. Moreover, as for the European Union's CE marking, the SRU/HRU-series breakers have obtained third-party certification from TÜV Rheinland. Therefore, machinery and equipment using these breakers can proceed smoothly through certification procedures in countries where the affixation of the CE mark is mandatory.

We have described the major features of the UL489-compliant SRU/HRU-series small-sized Molded Case Circuit Breakers along with the new technologies underlying these features. Looking ahead to the future, we are determined to develop products that are in keeping with the needs of our customers.

Table 2 Suitable standards and certification for countries

Area	USA	Canada	Europe	China	Japan
Applicable standard	UL489	CSA C22.2 NO. 5-02	EN 60947-2	GB 14048.2	JIS C 8201-2
State of compliance	○	○	○	○	○
Certification system	UL Label Service	cUL Label Service	CE Marking	CCC	–
Certification body	UL	UL	TÜV Rheinland	CQC	–

Improvement in Breaking Performance of UL489 Listed Compact Circuit Breakers of SRU/HRU Series

Author: *Takao Mitsuhashi**

We have developed a new arc-extinguishing system that makes it possible for small-sized circuit breakers to fulfill single-pole breaking duty at a rated voltage of 480 V as stipulated in the UL489 Standard. This arc-extinguishing system, which we have applied to SRU/HRU-series circuit breakers, adopts a linear-motion double-breaking system that excels in both interrupting performance in high-voltage circuitry and reduction of internal pressure buildup at the time of interruption and an arrangement to prevent a restrike caused by the pole-reclosing operation of the moving contactor.

1. Interruption Testing Specific to UL489 Standard

UL489-compliant circuit breakers are required to successfully pass not only three-phase interruption testing (HIC) but also satisfy sequence Z (given a rated voltage of 480 V, O-CO duty testing is performed at AC 480 V, 8.66 kA on a pole-by-pole basis and then three-phase O duty testing is done at AC 480 V, 10 kA). In this single-pole interruption testing, although the current to be interrupted is small when compared with other testing, the voltage that is applied across the contacts is high. For this reason, an arc-extinguishing system capable of restoring a high degree of insulation across those contacts becomes indispensable.

2. Linear-motion Double-breaking System

Figure 1 shows an internal construction diagram of a new-model circuit breaker employing a linear-motion double-breaking arc-extinguishing system. This circuit breaker features downsized dimensions made possible by adopting the said system and, thereby, approximately halving the stroke of the pressing plate (operation axis) when compared with that of a similar conventional single-breaking system.

Double-breaking systems can be divided into linear-motion and rotary-motion types, based on the type of contactor movement. As a rotary-motion type, there is the fork type. Since, in these double-breaking systems, electrode-fall voltage, which is two times higher than with comparable single-breaking systems, develops immediately after pole opening, the double-breaking systems lend themselves to the realization of high current-limiting performance. Shown in Fig. 2 are a prototype single-breaking and double-breaking circuit breakers' voltage waveforms that developed across the electrodes at the time of single-pole interruption at AC 480 V, 10 kA, in relation to the line-voltage waveform. As can be seen from the figure, the restriking voltage (approx. –200 V) that developed immediately after interruption in the double-breaking circuit breaker that features a faster inter-electrode voltage rise and shorter breaking time is smaller than its counterpart


Fig. 1 New low-voltage circuit breaker with linear-motion double-breaking system
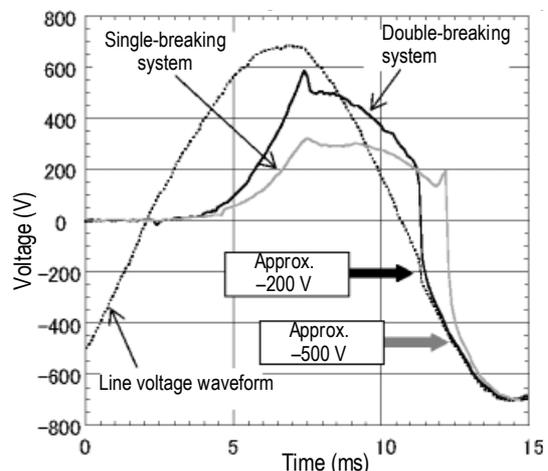
Fig. 2 Restriking voltages of double-breaking system and single-breaking system

* Advanced Technology R&D Center

(approx. –500 V) in the single-breaking circuit breaker. This indicates that the double-breaking system, which excels in current-limiting performance, has a smaller recovery rate of insulation characteristics, which is required between the electrodes immediately after interruption. The double-breaking system can, therefore, be advantageous in shutting off power in high-voltage circuitry.

3. Double-breaking "Polymer Ablation Type Auto-Puffer" Basic Testing

"Polymer Ablation Type Auto-Puffer", which is a proprietary technology of Mitsubishi Electric Corporation, enhances breaking performance in high-voltage circuitry. This particular technology is designed to cause a high-polymer material to produce ablation gas using the heat of an arc that occurs across the contacts at the time of interruption operation. The gas is trapped inside a chamber to be used to extinguish the arc by blowing the gas at it. The gas can enhance the recovery rate of insulation characteristics across the electrodes in the vicinity of current zero. Since this technology makes active use of the ablation gas, the internal pressure inside the chamber tends to build up at interruption time increasing the need to strengthen the chamber that bears up under that pressure. From the viewpoint of the strength of the chamber, the lower the rise of the internal pressure, the better. On the other hand, the higher the internal pressure generation, the more advantageous in the interest of shutting down power in high-voltage circuitry. Given this situation, in our development work this time around, we prototyped and evaluated basic model breakers by applying the "Polymer Ablation Type Auto-Puffer" to various kinds of arc-extinguishing systems. At the same time, we adopted a linear-motion double-breaking system that provides an excellent balance between interrupting performance in high-voltage circuitry and internal pressure rise at the time of interruption.

Table 1 shows the results of testing performed on the basic model breakers. We adjusted the peak value of intra-chamber pressure by varying the area of the exhaust ports. We defined a successful shut-down to be one that completes without restrike before the current zero point immediately after the first half wave, and compared intra-chamber pressure peaks determined at that time. In the case of the single-breaking model with an arc-extinguishing space of L40 × H23 × W17 mm, shut off was not possible even when we increased the intra-chamber peak pressure to 1.2 MPa. We, therefore, increased the intra-chamber space by 25% (to L50 × H23 × W17 mm) and succeeded in shutting off at an internal pressure of 0.49 MPa. On the other hand, in the case of the double-breaking model, we successfully achieved shut-off under all conditions that we set. This result attests to the fact that the double-breaking system has an edge over the aforementioned single-breaking system in shutting off power in high-voltage circuitry. Under the condition of keeping outer product dimensions in mind and a practicable maximum exhaust port diameter of 10 mm, the ratio between the linear-motion type (0.28 MPa) and the fork type (0.80 MPa) stood at approximately 1:3. Thus, the linear-motion double-breaking system is considered to be an excellent system for both ensuring unfailing shut-off performance in high-voltage circuitry and reducing the need to boost internal pressure at the time of interruption.

Table 1 Peak pressures of experimental models at short-current interruption (AC 600 V, 10 kA, pf 0.24)

Arc-extinguishing system layout	Double-breaking systems		Single-breaking system
	Linear-motion type	Fork type	
Basic experimental models			
Arc-extinguishing space dimensions	L55 × H23 × W17 mm	L40 × H23 × W17 mm	L40(50) × H23 × W17 mm
Internal pressure peak at the time of successful interruption	0.68 MPa (g=16 mm, d=5 mm) 0.28 MPa (g=16 mm, d=10 mm)	0.80 MPa (g=16 mm, d=10 mm)	0.49 MPa (g=16 mm, d=10 mm) where L=50 mm
Min. inter-contact distance at the time of successful interruption	7 mm × 2 (6 mm × 2 at AC 480 V)	10 mm × 2 or less	16 mm
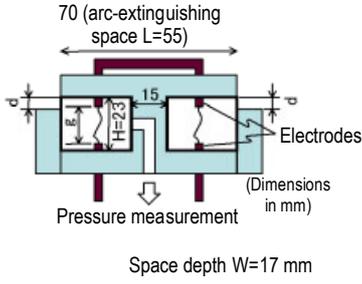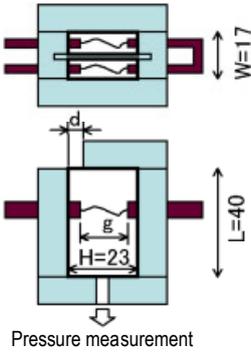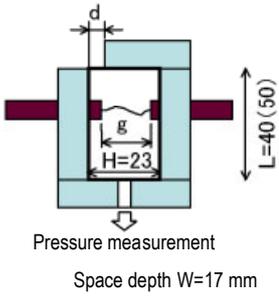
4. Impact of Contact Materials on the Recovery Rate of Insulation Characteristic

In the case of circuit breakers adopting "Polymer Ablation Type Auto-Puffer," a stream of gas is used to extinguish an arc that lasts by means of conductive vapor supplied from the arc spot. Therefore, the recovery rate of insulation characteristics is impacted by the electrode material with which the arc spot is formed. Given this situation, using a single-breaking system and various kinds of electrode materials (such as iron, copper, and various silver-containing contact materials), we made comparisons of peak internal pressures required for achieving successful shut-offs. As a result, we found out that some silver-based materials called for higher peak internal pressures than copper and iron to successfully achieve shut-offs.

To work around this problem in the new-model circuit breaker, we provided a large-sized arc runner and arc horn, both made of copper, with which to displace the arc spot occurring across the contacts in order that no arc spot is formed at the contacts at arc-extinguishing time. By virtue of this arrangement, we achieved a system that renders interruption performance unaffected by the material of the contacts.

5. Restrike Prevention Technology

Just like at the time of short-circuit-caused interruption, the contacts open also at the time of sequence-z single-pole interruption due to inter-contact electromagnetic repulsion before the mechanism section starts its pole-opening operation. Since this pole-opening electromagnetic force sharply attenuates following a current peak, the moving contactor begins pole-reclosing operation at the instant when the contact spring's pole-closing force becomes greater than the electromagnetic repulsion. Since this pole-reclosing operation proceeds until the pressing plate causes the moving contacts to open by the mechanism section's motion, a restrike occurs between the contacts as a result of single-pole interruption's high restriking voltage if the mechanism section's motion is slow, reducing the contact-to-contact distance in the vicinity of the current zero point. In the case of single-pole interruption, since the operating speed of the tripping section that actuates the mechanism section becomes relatively slower when compared with short-circuit-caused interruption because the current to be interrupted is lower, it is impossible to expect the mechanism section to perform high-speed contact-opening operation. To cope with this, in the case of the new-model circuit breaker, we increased the pole-opening electromagnetic force during the latter half of breaking operation in order to defer the time to start pole-reclosing operation so that a sufficiently large contact-to-contact distance can be secured for interruption at the current zero point.

UL489 Listed Molded Case Circuit Breaker "NF50-SMU" Series

Authors: *Hisashi Yamanaka*[*] and *Yasuhiro Ashikari*[*]

In recent years, molded case circuit breakers that are compliant with UL489 standard need the smaller breakers for the purpose of installing multiple units in branch circuits. In a bid to respond to such a need, we have developed NF50-SMU-series UL489 listed molded case circuit breaker. This paper describes the major features of the series and our incorporated breaking-current-limiting technologies.

1. Features of the Newly Developed UL489 Listed Molded Case Circuit Breakers

As distinctive characteristics of the UL489 Standard, we cite the following two points:
(1) Large values are specified for insulation clearance between the terminals of dissimilar poles.
(2) Single-pole breaking operation duty is strict.

As shown in Table 1, the NF50-SMU-series UL489 listed molded case circuit breaker (Fig. 1) have the following features:

1.1 Reduced Housing Dimensions and Broadened Assortment of Single-pole Breakers

When compared with our earlier UL489 listed 50-ampere frame models, the NF50-SMU series features considerable reduction in width from 25 mm to 18 mm and in volume from 100% to 44% per single-pole model by virtue of enhanced breaking-current-limiting performance, which we discuss later on, thus contributing to savings in space on panelboards of machinery, equipment and the like.

Although we offered only 3-pole and 2-pole models in the past, we have established a single-pole model line to enable installation in circuits that stand in need of single-pole breakers only.

1.2 High Breaking Capacity of Small-sized Model

The Semiconductor Equipment and Materials International Standards (SEMI) of the chipmaking industry include a breaking-capacity requirement of 10 kA for circuit breakers to be installed. In the case of the NF50-SMU-series breakers, we have achieved this high breaking capacity of 10 kA by dint of the enhanced current-limiting performance.

To achieve a high breaking capacity in the face of the small outer housing dimensions of a circuit breaker, the ability to withstand energy that passes through the tight space inside the circuit breaker at the time of a high-current interruption is essential. To minimize

Fig. 1 UL489 Listed Molded Case Circuit Breaker "NF50-SMU" Series

Table 1 Specifications

Model			NF50-SMU		
Number of poles			1	2	3
Rated current I_n [A]			0.5, 1, 1.5, 2, 3, 4, 5, 6, 7, 8, 10, 13, 15, 20, 25, 30, 35		
Rated breaking capacity [kA]	UL489 CSA C22.2 No. 5	AC120V (Δ)	10	–	
		AC240V (Δ)	–	10	
		AC60V	10	–	
	IEC60947-2 JIS C8201-2 (I_{cu}/I_{cs})	AC230V	10/7.5	–	
		AC400V	–	10/7.5	
		AC60V	10/7.5	–	
Overall dimesions [mm]		a	18	36	54
		b	124		
		c	44		
		ca	70		
Accessory devices			Alarm switch, auxiliary switch, shunt trip device, and handle lock device		
Conforming standards			UL489, CSA22.2 No. 5, IEC60947-2, JIS C8201-2		

damage to the circuit breaker, it is necessary to enhance current-limiting performance and, thereby, reduce the energy that passes at breaking time to a minimum.

The NF50-SMU series adopts an arc movement type: an arc that develops between contacts at the time of interruption is extended by means of rail-like electrodes and is broken by an arc-extinguishing device. This arc movement type is combined with the following two internal structural features to enhance current-limiting performance with which to reduce the energy that passes through at the time of interruption.

(1) High-speed forced opening under the effect of an electromagnetic coil

By forcibly separating the moving contact from the stationary contact at high speed under the force of the electromagnetic coil for instantaneous tripping purposes, it has become possible to shorten the time required until arc movement begins. As shown in Fig. 2, there is a need to reduce the maximum current I_p that passes through the circuit breaker; the solution is to find ways of reducing the time td (dead time) until the commencement of arc movement. The slight difference in time between td1 and td2 translates into the difference in current value between I_p1 and I_p2. In the end, this difference in current produces a reduction in the amount of let-through energy that is represented by the hatched area. In other words, it produces a large difference in current-limiting performance. The td represents a value in time, say within an extremely short length of a few milliseconds, meaning that a reduction of the order of a millisecond has immense significance.
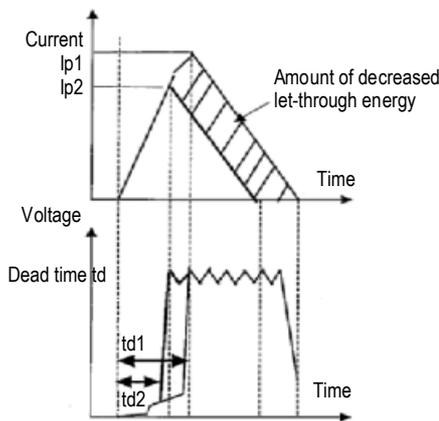
Fig. 2 Current-limiting waveform

(2) Uniformization of exhaust

In order that gas that has evolved at the time of interruption is discharged uniformly, we have provided exhaust ports in multiple places. This provision makes it possible to stably maintain the arc voltage subsequent to arc movement and it has become possible to interrupt high breaking current.

As explained above, since there is no need to se-

cure large clearance between contacts, unlike a non-arc movement type, high-current interruption is possible in a small space.

Figures 3 and 4 show comparisons between our earlier and newly developed breakers in terms of peak let-through current value I_p and let-through energy I^2t.
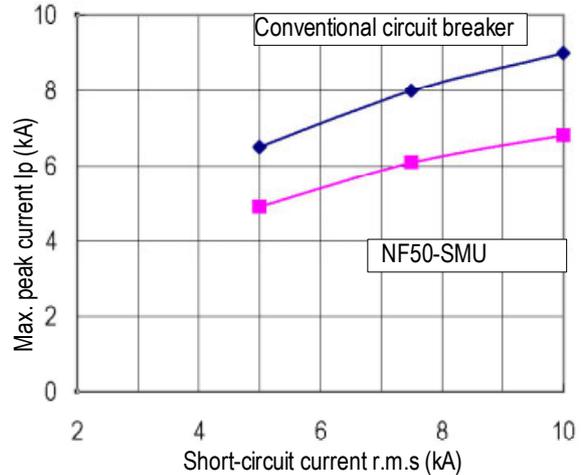
Fig. 3 Current-limiting characteristics comparison (AC220V)
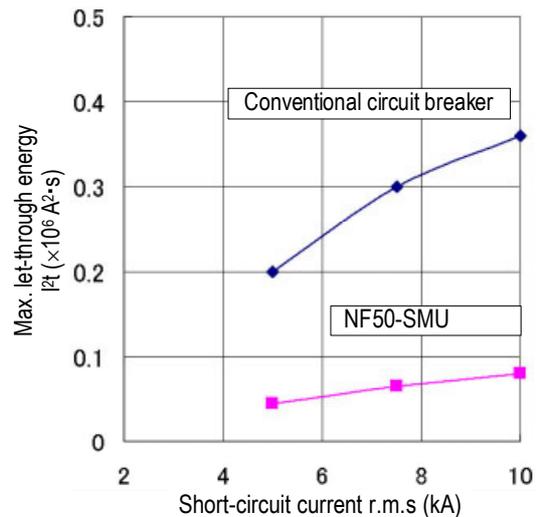
Fig. 4 I²t let-through characteristics comparison (AC 220 V)

1.3 Conformity of Several International Standards

Export-oriented equipment manufacturers must meet the need for sets that may be used anywhere in the world. Given this situation, the need for adherence to various international standards has also been growing in the field of circuit breakers that make their way into panelboards.

The NF50-SMU-series breakers conform to the circuit-breaker portions of the world's major standards, namely the U.S.'s UL, Canada's CSA, the EU's IEC and Japan's JIS Standards. What is more, we printed the pertinent numbers of these standards on the breaker housings.

1.4 Lower Rated Current with Thermal-magnetic-type Breakers

The smallest current rating of our conventional UL489 listed molded case circuit breakers of the thermal-magnetic type was 15A. By virtue of the following two measures, we have expanded the lower end of the current-rating range down to 0.5A.

(1) The tripping load of the mechanism to trip the main body has been reduced. This has resulted in the reduction of the operating load of the bimetal, enabling lower-rated-current thermal operation.

(2) Structural provision has been made to prevent current from flowing through the bimetal and coil after completion of arc movement that takes place at the time of interruption. This provision lightens the load on the bimetal and coil at the time of interruption, which in turn has resulted in high breaking capacity in low-rating breakers.

In the case of our earlier circuit breakers rated at 15A or less, the operating characteristics of the available hydraulic-magnetic-type units were affected by the installation orientation. Since the NF50-SMU-series breakers are of the thermal-magnetic type that are immune to their installed position, users can choose from a broader circuit-breaker assortment.

1.5 Add-ons Made Available

As add-ons to the NF50-SMU-series breakers, an alarm switch (AL), an auxiliary switch (AX), a shunt trip device (SHT), and a handle lock device (HL) are available. The alarm switch, auxiliary switch, and shunt trip device are designed to permit installation on either side of the breaker housing.

1.6 Open/Close Terminal Covers Attached as Standard & AC/DC Two-way Operation for Single-pole Breakers

Covers that can be opened/closed are provided as standard over the line-side and load-side terminal portions of the breaker housing. These terminal covers feature a finger-protection construction pursuant to Finger Protection Class IP20 of the IEC Standards for increased safety.

The single-pole breakers are of the AC/DC two-way type and can be used in 230V-and-lower AC circuits and 60V-and-lower DC circuits.

We have described the features of the NF50-SMU-series UL489 listed molded case circuit breaker and the current-limiting technologies incorporated in them. Down the road, we will continue developing and offering NF50-SMU-series breakers that better address customer needs.

Measuring Unit for MDU Breaker

Authors: *Haruhiko Yamazaki** and *Kenichi Haramoto**

1. Foreword

An "MDU breaker" is a circuit breaker incorporating VTs and CTs for measurement purposes and is capable of monitoring a circuit in combination with a measuring display unit (MDU). In other words, this product features savings in installation work and space. However, in recent years, we have seen an increased need for the following: (1) Reduction in per-measurement-item cost, (2) Retrofitting of MDUs, and (3) Support for offline logging, CC-Link communications, LonWorks communications and the like. To address these needs, we have developed a range of Measuring Units for MDU Breakers (code-named "MDU2").

2. MDU Breakers

When compared with an arrangement combining measurement equipment with external VTs and CTs, MDU breakers have the following features:

- Savings in installation work, wiring and space
- Installation is possible in a space just large enough for a conventional circuit breaker.

What is more, measurement and monitoring are performed on circuit-breaker-specific information such as: load-current Pre-Alarm (PAL) stored in the circuit breaker itself, overcurrent alarm (OVER), and cause of fault and fault-current measurement results in the event that the circuit breaker trips. By virtue of the above, the following are also possible:

- Monitoring of circuit, fault prevention and equipment maintenance

2.1 MDU Breaker Composition

MDU breakers range from 225A to 800A frame.

The MDU2 lineup consists of 4 variations in measurement circuit count and communication scheme. Table 1 shows measurement items and monitor items that can be implemented when MDU breakers are combined with each of the MDU2 variations. As for the internal composition of the typical MDU breaker, a measurement-purpose CT is installed on each individual phase in such a manner that a resistor/CT series circuit is placed across Phases 1 and 2 and another resistor/CT series circuit is placed across Phases 2 and 3 as voltage detection VTs. These provisions are intended to isolate signals going to the MDU2 from the main circuit and, thereby, ensure safety. The outward appearance of the MDU2 is shown in Fig. 1. Below, we describe the internal composition of the MDU2 by taking a look at the block diagram shown in Fig. 2. Signals from MDU breakers are level-converted at the input circuitry and fed into the respective measurement-use CPUs. Current and voltage analog signals are analog-to-digital converted and various measurement values are worked out. On the other hand, alarm signal circuitry continually monitors variations in level. Calculated-value data and alarm-status data deriving from each measurement-use CPU are internally transferred to the unit's CPU. Since the unit's CPU has a pair of internal communications lines, it sends out the required data in response to requests from a display unit and external communications. Since each measuring section is modularized, measurement of up to seven circuits is possible through the addition of submodules. Furthermore, the communications section is also modularized to support various kinds of communications.

Table 1 Lineup of MDU2s. Measurement item for monitoring and communication

|			3 circuits		5 circuits	7 circuits
			MDU2-3-L	MDU2-3-C	MDU2-5-C	MDU2-7-C
Measurement items		Load current	○	○	○	○
		Line voltage	○	○	○	○
		Harmonic current	○	○	○	○
		Power	○	○	○	○
		Active energy	○	○	○	○
		Reactive power	○	○	○	○
		Reactive energy	○	○	○	○
		Power factor	○	○	○	○
		Frequency	○	○	○	○
		Fault current	–	○	○	○
Monitoring		Pre-alarm	–	○	○	○
		Overcurrent alarm	–	○	○	○
Communications		CC-Link communications	–	○	○	○
		LonWorks® communications	○	–	–	–
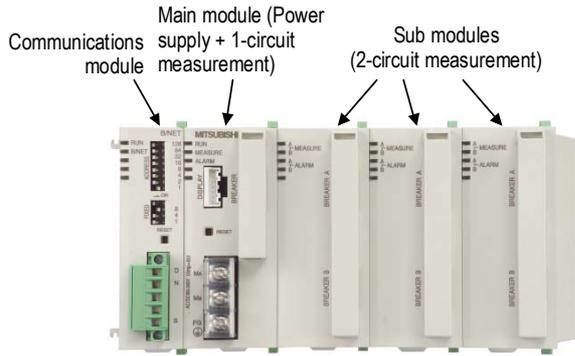
Fig. 1 Outline of MDU2
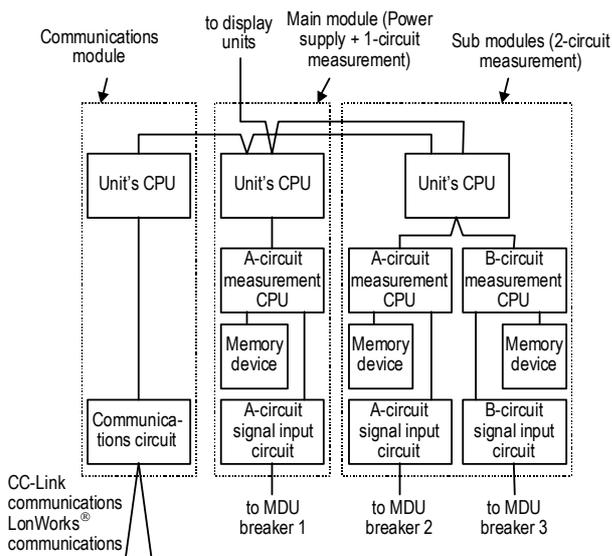
* As an example, a 3-circuit measurement configuration is shown. (Power supply circuitry is omitted for brevity.)

Fig. 2 Block diagram of MDU2

3. Technologies Employed to Enhance the Precision of Measurements Made at the MDU2

MDU breakers' measurement-use VTs and CTs have been downsized in order to permit installation in breakers. For this reason, they are inferior to ordinary VTs and CTs for use with meters in terms of tolerance, linearity and phase characteristics and stand in need of being corrected by the measurement-use CPU. Moreover, since the characteristics of these downsized VTs and CTs vary widely, it is necessary to perform adjustment testing on a breaker-by-breaker basis and determine correction values. In the past, corrections were carried out at a mere three points or so in spite of the fact that measurement-use CTs vary widely in phase error under light load. Since no measures have been taken to cope with this variation, there has been a problem in that the required measurement precision cannot be satisfied when using a combination different from the one on which adjustments were made. To solve this problem, we have increased the number of correction points in the region below 20% of the rated

capacity in order that finer corrections can be made. Figure 3 shows an example of a comparison between the results of past corrections and the results of corrections made this time.

As a result, the precision of electric energy measurements has been enhanced from ±2.5% of the rated capacity to ±2.5% of true values in the 5%-to-100% current range.
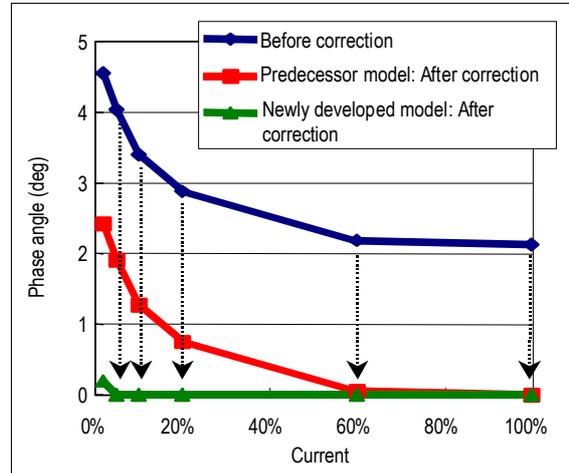

Fig. 3 Characteristics of revised phase lag in CT

4. Automatic Recognition of MDU Breakers

Since various MDU breakers may be connected to the individual input circuits of the MDU2, automatic recognition capability is required. Given this situation, it became necessary to provide a means of storing correction values on the MDU breaker side for the following reasons:

- In relation to the A frame of a given MDU, the ratio of its CTs is required to be changed.
- The errors of the VTs and CTs for measurement use incorporated in a given MDU breaker are unique to that particular MDU breaker.

To realize the means and solve the problem, we installed a memory device on the MDU breaker side to store the following items of information: A-frame, model designation and correction values for CTs and VTs.

5. Example of Connections Between MDU Breakers and MDU2

Figure 4 shows an example of connecting multiple MDU breakers to an MDU2. A single MDU2 is capable of performing measurements on multiple transformer systems (with dissimilar voltages and phase lines). The length of the cable between each MDU breaker and the MDU2 can be up to 10 m long. If the number of measurement items is limited and the distance between measurement points is long, it is possible to provide support using an integral-type MDU breaker and transmit circuit information over a network. What is more, the

display-unit lineup includes one logging display unit capable of collecting and accumulating log data to enable off-line logging. As discussed above, these units can be flexibly configured to meet the particular needs of each customer in accordance with his system.

6. Conclusion

For the future, we are committed to improving upon the MDU breakers and MDU2 that are characterized by the features discussed above while setting our sights on downsizing, greater functionality and reduction in price.
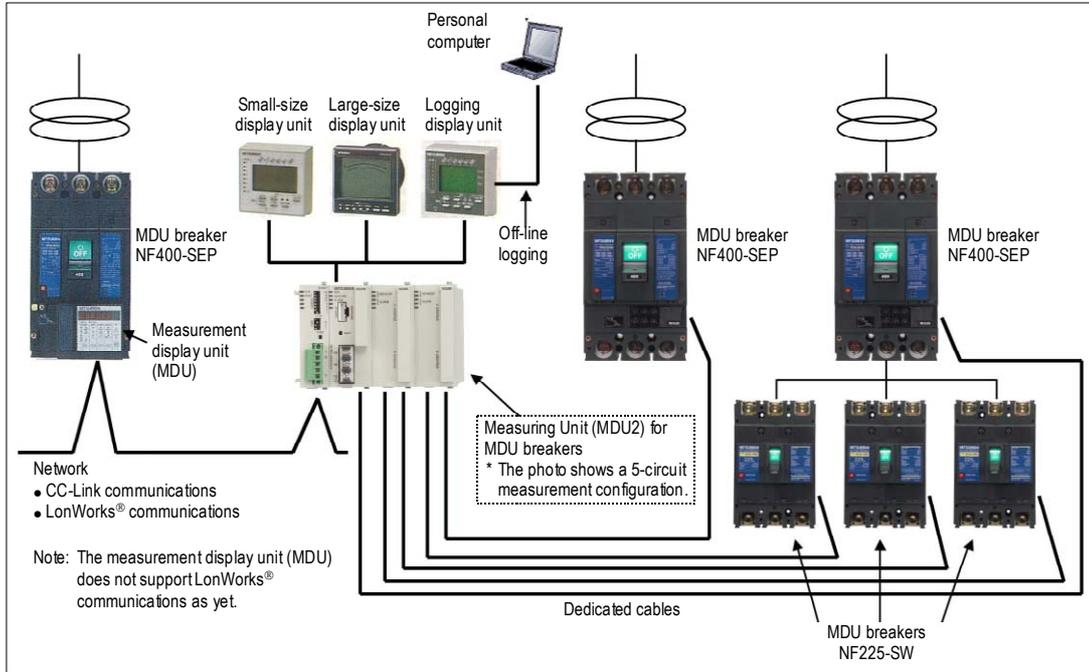

Fig. 4 Example of connection of MDU Breaker and MDU2

Responding to the RoHS Directive and Technology for Low Voltage Circuit Breakers

Authors: *Setsuo Hosogai*[*] and *Hitoshi Ito*[*]

Abstract

In this paper, we discuss the reliability of our RoHS-compliant low-voltage circuit breakers and our efforts at developing electrical contact materials. In preparation for the adoption of lead-free soldering, we made thermal fatigue life predictions for surface-mounted parts by means of experimental inspection and CAE analysis. As for hexavalent chromium-free materials, we confirmed their reliability through practical product verification. Furthermore, we have established a technology to obviate the need for cadmium in electrical contacts.

1. Our Efforts to Achieve Conformity to RoHS

In Europe, the RoHS Directive (Restriction of the Use of Certain Hazardous Substances in Electrical and Electronic Equipment Directive) comes into effect on July 1, 2006.

The following six substances are specified as hazardous substances: lead, hexavalent chromium, cadmium, mercury, polybrominated biphenyls (PBB) and polybrominated diphenyl ethers (PBDE). However, there are also exemptions from the application of the Directive, including hard-to-replace substances such as lead contained in free-cutting alloys. Furthermore, cadmium compounds contained in electrical contacts are being considered for possible exemption from the Directive.

Just as is the case with electrical and electronic equipment in general, lead is contained in low-voltage circuit breakers, specifically in solder joints of electronic parts mounted on printed circuit boards as well as in solder-joined electrical connections. In addition, hexavalent chromium is contained in chromate conversion coatings of zinc-coated parts where galvanization is employed as a rust-preventing process for parts made of steel. What is more, there are cases where cadmium compounds are contained in electrical contacts.

Mitsubishi Electric Corporation has been making active efforts at reducing the load on the environment. In 2004, the company achieved conformity to the RoHS Directive with the then newly developed UL489-compliant SRU/HRU-series small-sized circuit breakers.

With January 2006 as a target date, the company is currently making stepped-up efforts at bringing the entirety of its low-voltage circuit breakers into RoHS Directive compliance.

In this paper, we report three constituent technologies we are using to achieve conformity to the RoHS Directive.

2. Thermal Stress Life of Lead-free Solder Joints

In low-voltage circuit breakers, we have been using Sn-Pb solder in solder joints of electronic parts mounted on printed circuit boards as well as in solder-joined electrical connections.

Low-voltage circuit breakers are important pieces of equipment used for the protection of low-voltage indoor circuits and are generally required to have a long life span of 15 years.

Given this situation, to achieve the elimination of lead from solder, we have adopted Sn-Ag-Cu solder that boasts the highest reliability among the various kinds of lead-free solders and has a track record of being adopted into industrial-use equipment.

Figure 1 shows a printed circuit board to be built inside low-voltage circuit breakers. It is populated with SOPs (Small Outline Packages), chip capacitors, cylindrical resistors and the like.

In the marketplace or out in the field, thermal stress caused by the difference in thermal expansion coefficient between the base materials of these parts and the printed circuit board is applied to the solder joints under temperature cycling.

Since the Sn-Ag-Cu solder differs from traditionally used solder in terms of mechanical properties such as modulus of elasticity in tension and creep characteristic, we predicted that the solder joints' thermal-fatigue life would change under repeated applications of thermal stress.

To make thermal-fatigue life predictions, we continuously measured the electrical resistance of the

solder joints of individual parts in temperature cycle testing and counted the number of cycles it took for each individual solder crack to develop.

It is known that a logarithmic plot of a test temperature range ΔT (or generated strain) and the solder-crack life of a given solder joint can be represented by a quasi-linear approximation. By using this, we estimated thermal-fatigue life in an assumed environment in the market.

Figure 2 shows an example of the results of testing we performed on cylindrical resistors.

The testing confirmed that the lead-free solder crack life of the individual parts had sufficient margins in relation to the assumed environment in the market.

On the other hand, among a broad product range of low-voltage circuit breakers, there are cases in which parts with dimensions that differ from those of the parts used for the testing are used in such circuit breakers.

For such cases, we made thermal-fatigue life predictions by calculating generated strain by means of CAE-based nonlinear elastic-plastic creep analysis and by using the above-mentioned life prediction line. As a result, we have verified that lead-free soldering has adequate service life margins for use in the assumed environment out in the field.

3. Reliability of Hexavalent Chromium-free Materials

Our low-voltage circuit breakers use steel parts such as switching mechanism components, terminal screws, and a magnetic iron plate that is called a grid and used in the arc-extinguishing chamber. As a rust-preventing process for those parts, we have been using zinc plating called chromate conversion coatings.

Chromate conversion coatings represent the most prevalently practiced rust-preventive measure for iron and steel parts. Zinc plating has a rustproofing function to prevent iron from rusting while chromate conversion coatings have a function to prevent the chromate conversion coatings from corrosion under corrosive environments.

Since these chromate conversion coatings contain hexavalent chromium compounds, chromate chemical producers and zinc-coated steel sheet manufacturers began developing hexavalent chromium-free coatings several years ago.

At the outset of adopting hexavalent chromium-free coatings for zinc-coated parts and zinc-coated steel sheets to be used in the low-voltage circuit breakers, we conducted verification tests under such headings as anti-corrosivity and bolted-joint characteristics. Eventually, we adopted trivalent chromium chromate conversion coatings for zinc-coated parts and chromium-free coatings for zinc-coated steel sheets (See Table 1).

Table 1 Chromate and Hexavalent chromium free conversion coatings

Classification	Chromate conversion coatings	Hexavalent chromium-free coatings
Zinc-coated parts	Chromate conversion coating (Hexavalent chromium compound)	Trivalent chromium chromate conversion coating (Trivalent chromium compound+additives)
Zinc-coated steel sheet	Special chromate conversion coating (Hexavalent chromium compound)	Chromium-free coatings (Organic compound costing)

4. Development of Cadmium-free Electrical Contacts

The low-voltage circuit breakers' electrical contacts, to which the heavy load of breaking arcs is applied at the time of opening, are required to possess low electrical resistance, welding resistance and erosion resistance under repeated switching operations. To meet these requirements, composite materials as prepared by adding oxides, carbides and graphite (which combine to enhance resistance to welding and erosion) to silver (which features low contact resistance) are being employed for the manufacture of electrical contacts.
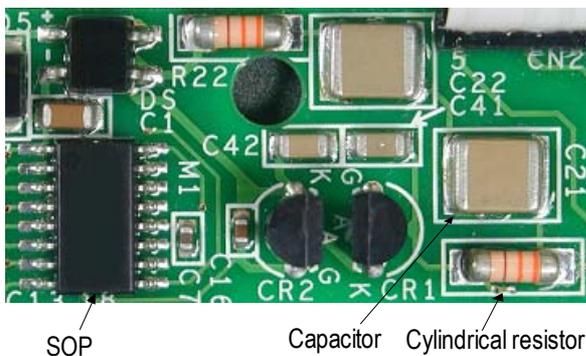

**Fig. 1 Example of printed circuit board in low-voltage circuit breaker**
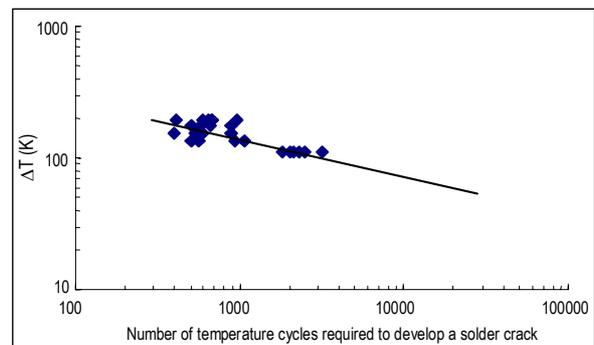
Fig. 2 Solder crack lifetime of cylindrical resistor

For some of our low-voltage circuit breakers, we have been using Ag-CdO contacts. Under the RoHS Directive, although cadmium compounds contained in electrical contacts are under consideration for possible removal from the list as hard-to-replace applications, we have been working on the development of cadmium-free contacts in collaboration with our contact vendors in an effort to reduce the load on the environment by taking the opportunity to bring our products into conformance with the RoHS Directive.

As for the preparation of our newly developed cadmium-free material, trace amounts of various compound additives are blended with a base material that is made by adding Sn compound and In compound, in place of CdO, to Ag. What is more, we are able to control the structure in the production processes. By virtue of this material, it has become possible for us to switch over to cadmium-free contacts.

Above, we discussed the constituent technologies that enabled us to bring our low-voltage circuit breakers into conformance with the RoHS Directive. In the future, those at Mitsubishi Electric Corporation involved in the R&D of low-voltage circuit breakers are committed to making active efforts at reducing the environmental load.

MITSUBISHI ELECTRIC CORPORATION

HEAD OFFICE : MITSUBISHI DENKI BLDG., MARUNOUCHI, TOKYO 100-8310. FAX 03-3218-3455